A NUMERICAL-EXPERIMENTAL STUDY OF THE AIR ENTRAINMENT FOR SELF ASPIRING BURNERS

L. S. Baldani,

and P. S. B. Zdanski

Universidade do Estado de Santa Catarina

Departamento de Engenharia Mecânica

Centro de Ciências Tecnológicas

Bairro Zona Industrial Norte

CP. 98219-710, Joinville, SC, Brasil

baldanils@gmail.com

paulo.zdanski@udesc.br

ABSTRACT

This work presents an experimental and numerical study addressing the effects of air entrainment for self aspiring burners. Within this framework, the work focus on the analysis of four different burners tested with four different nozzles, resulting in a total of sixteen different configurations. The gas used for the tests was methane. Each nozzle diameter provided a different flow rate, which also resulted in a different entrainment, therefore a different oxygen concentration on the ports area, which was measured using an oxygen sensor. The level of oxygen decreased with the increase of the flow rate of the gas, and had a linear behavior with the nozzle diameter. The finite volume method with the realizable k-ε model was then applied to numerically investigate this phenomenon using the commercial software STARCCM+. The results shows that for the sixteen points tested the worst correlation had a relative error of 2.95%, while for the best one was of 0.04%.

NOMENCLATURE

ANOVA	analysis of variance
$\overline{C}_Y$	average concentration for the specie Y
$\overline{C_Y'}$	average concentration fluctuation for the specie Y
$\overline{p}$	average static pressure, Pa
$\overline{S}_{ji}$	average stress tensor, s^{-1}
$\overline{u}_j\ \overline{u}_i$	average velocity component on the j and i direction, m/s
$\overline{u_j'}\ \overline{u_i'}$	average velocity fluctuation component on the j and i direction, m/s
d	diameter of a circular nozzle, mm
D_{AB}	diffusion coefficient of the specie A into B, m^2/s
δ_{ij}	Kronecker operator
l_0	length scale, mm
$\dot{m}$	mass flow rate, kg/s
h	nozzle to target distance, mm
k	turbulence kinetic energy, m^2/s^2
O_2	oxygen
M_{Lab}	O_2 mole fraction obtained experimentally
M_{CFD}	O_2 mole fraction obtained numerically
τ_{ij}	Reynolds stress tensor, Pa
i, j	sub-indices of the transport equation
t	time, s
v_0	velocity scale, m/s
$x_j\ x_i$	Special component on the j and i direction, m
w.c	water column

Greek symbols

α	alpha risc
ε	dissipation rate, m^2/s^3
μ	viscosity of the fluid, Pa·s
μ_T	turbulent viscosity, Pa·s
ρ	density of the fluid, kg/ m^3
σ	standard deviation

INTRODUCTION

Self aspiring burners are very common in household's appliance in Brazil. Its fuel source can vary, being one of them the natural gas, that is mainly composed by methane (Faveri, 2013), as shown in Fig. 01.
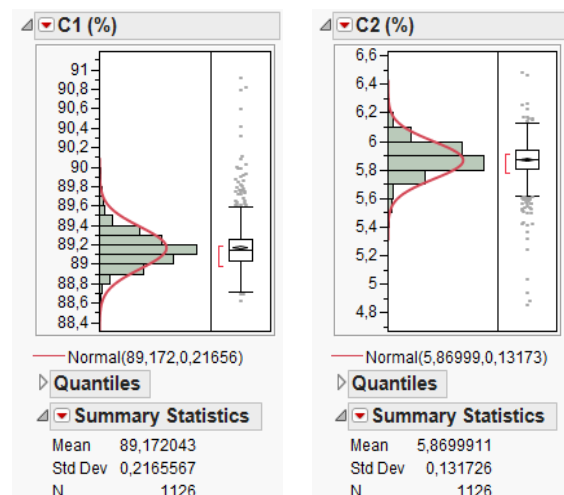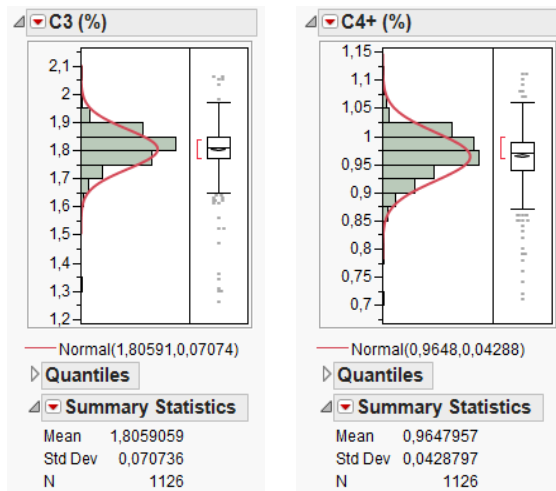
Figure 01. Distribution of the components C1 (methane), C2 (ethane), C3 (propane), C4+ (components with more than 4 carbons).

The primary air or entrainment is responsible for several flame effects such as (Glassman & Yetter, 2008): flame velocity, flashback (when flame velocity is higher than the mixture flow), lifting (when flame velocity is lower than the mixture flow), yellowing (result of carbon burning due to incomplete combustion) as well as carbon monoxide (CO) formation.

The CO formation is strictly regulated, in Brazil for domestic burners the maximum production is of 1000ppm (NBR13723-1, 2003). Therefore, the better the understanding of the entrainment phenomenon, the better is the burner development.

The entrainment is caused due to the discharge of a free fuel jet into the environment. The jet spreads conically, losing velocity and entraining gas from the surroundings (Field *et al.*, 1967), Fig. 02.

The study of free jets is large applied. They can be air-air, air-water, air-methane (as in this study), etc. The study of the influence of the geometry on the jet and its characteristics can also be found in the literature. (i) Kim & Park (2013) performed a numerical investigation of the effect of noncircular inlet for the jet, analyzing a square and triangular shape that presented a more vigorous secondary flow when compared with the circular nozzle; (ii) Singh *et al.*, (2003) investigate experimentally the entrainment for a circular e non circular jets being them confined and semiconfined, for the noncircular jets the one with the isosceles triangle cross section resulted in the highest entrainment, for both the circular and noncircular the entrainment increased when the jet was moved away from the tube inlet; (iii) Singh (1999) developed a finite element model to predict the entrainment and mixing of a confined turbulent jet of variable density, the results were compared with the analytical solution; (iv) Pritchard *et al.*, (1977) proposed a formulation using the momentum and energy conservation for the mixing process of a jet inside a circular tube.
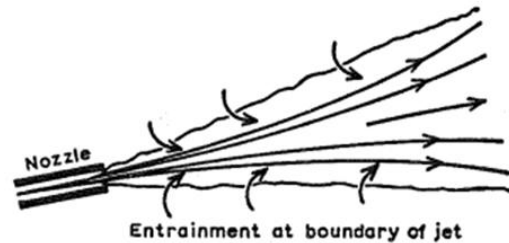

Figure 02. The free jet.

The prediction of the primary air is important on the determination of the flame effects. Its prediction was determined by several authors through (v) Carrillo Ibañez (2013) compared the turbulence models k-ε and SSG on the commercial software CFX to predict the jet velocity profiles, although none of them matched the measurements, the SSG model was chose to develop his burner design methodology due to the better convergence, even with the better results presented by the k-ε model; (vi) Namkhat & Jugjai (2010), presented a model for the primary air aeration both for the cold test as for the hot test, for the comparison of the model the authors used data obtained from laboratory measurements where a PIV and oxygen sensor was used to raise the data.

The main focus of the present work was to compare the experimental concentration of oxygen, on the ports area, with the values obtained with a commercial CFD code STARCCM+. For all the points compared, the one that presented the worst correlation had a relative error of 2.95% while for the best one was of 0.04%. The relative error was calculated by:

$$\frac{|M_{Lab} - M_{CFD}|}{M_{Lab}} \qquad (1)$$

EXPERIMENTAL METHODOLOGY

The experimental setup used in the present work is showed in Figs. 3 and 4. The burner was assembled in the test rig and connected to the fuel line. Each of the four burner types tested had their injector changed. The injectors were of a circular cross section with the diameters of 0.64 mm, 1.1 mm, 1.6 mm and 2 mm.
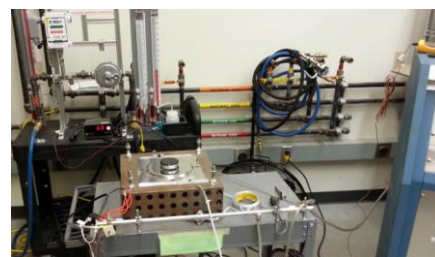

Figure 3. Photo of the test rig.

During the tests a pressure regulator (2) was used to control the gas pressure on the exit of the fuel tank (1). The value of 5" w.c was set, which could be verified by the manometer (4). Once that the gas exits the nozzle it promotes the entrainment on the burner (5) by the sharing of momentum with the ambient air. An oxygen sensor (6) positioned at the ports area was used to obtain the values of the mole fraction of O_2, displayed on the gas analyzer (7). Upon the stabilization of the concentration its value was then write down along with the flow rate (3).

Natural gas was used as fuel for the experiments. The tests had a total of 48 runs, each of the 16 sets of burners/injectors was tested 3 times. The burners were manufactured through several processes: aluminum injection (burner 1 and 4), conformation (burner 2) and machining (burner 3). An average of the measurements for each set was taken and with the use of the ANOVA analysis an estimated accuracy was obtained.
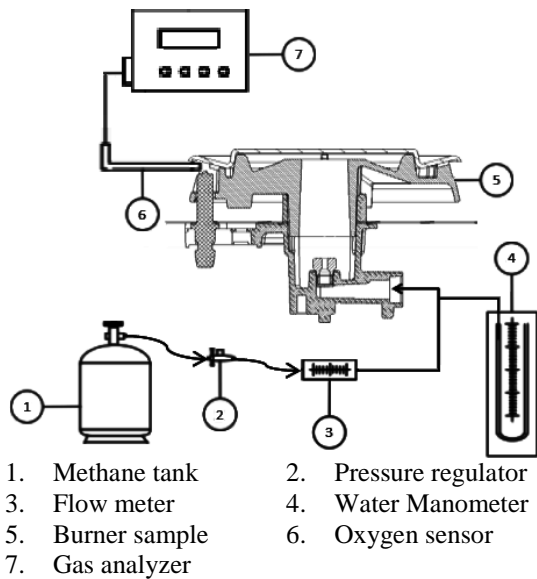

1. Methane tank   2. Pressure regulator
3. Flow meter   4. Water Manometer
5. Burner sample   6. Oxygen sensor
7. Gas analyzer

Figure 4. Schematic representation for the O_2 measurement.

The realization of those tests was similar in the materials and methods used by Namkhat & Jugjai (2010), except for the fact that no PIV measurement was tacked, for the cold tests.

The two variables recorded: fuel flow, used as boundary condition, and O_2 mole fraction, confrontation value, are fundamental for the validation of the numerical code.

NUMERICAL STUDY

The numerical study was conducted in order to determine whether the two-equation turbulence model realizable k-ε can help on the entrainment prediction close to experimental results. One of the computational domains for the present problem is

shown in Fig. 5. In this study, the flow is assumed to be three-dimensional, incompressible, steady and turbulent. Both gases, air, that was considered to be composed as 79% Nitrogen and 21% Oxygen in mole fraction, and methane are considered to be ideal gases. Chemical reactions are neglected.

Governing Equations

Reynolds averaged Navier-Stokes equations are used to model the turbulent flow. The time average continuity, momentum and species equations solved in the present are given below (Wilcox, 1998; Kays *et al.*, 2005).

$$\frac{\partial}{\partial t}\left(\rho\bar{u}_i\right) + \frac{\partial}{\partial x_j}\left(\rho\bar{u}_j\bar{u}_i\right) = \\ -\frac{\partial\bar{p}}{\partial x_i} + \frac{\partial}{\partial x_j}\left(2\mu\bar{S}_{ji} - \rho\overline{u'_j u'_i}\right) \tag{2}$$

$$\frac{\partial}{\partial x_i}\left(\bar{u}_i\right) = 0 \tag{3}$$

$$\frac{\partial}{\partial t}\left(\bar{C}_Y\right) + \frac{\partial}{\partial x_i}\left(\bar{u}_i\bar{C}_Y\right) = \\ \frac{\partial}{\partial x_i}\left(D_{AB}\frac{\partial\bar{C}_Y}{\partial x_i} - \overline{u'_i C'_Y}\right) \tag{4}$$

In order to close equation (2) the Boussinesq hypothesis is used,

$$\tau_{ij} = -\rho\overline{u'_j u'_i} = \mu_T\left(\frac{\partial\bar{u}_i}{\partial x_j} + \frac{\partial\bar{u}_j}{\partial x_i}\right) - \frac{2}{3}\delta_{ij}\rho k \tag{5}$$

The turbulent viscosity is usually expressed as

$$\mu_T \propto v_0 l_0 \tag{6}$$

where v_o and l_o are the velocity and length scales respectively. To obtain this variables are used the turbulent quantities k and ε. In this work the two-equation turbulence model used was the realizable k-ε, due to the fact that this model presented an increase on the prediction of flow recirculation when compared to the standard k-ε (Shih *et al.*, 1995).

For all the analysis the default model constants provided in STARCCM+ 10.02 were used. To capture the near wall effects the "all wall y+ treatment" was used for the realizable k-ε model (CD-adapco, 2015).

Boundary Conditions

Due to the symmetric geometry the boundaries conditions imposed to the model are presented on the Fig. 5 and goes as follow:
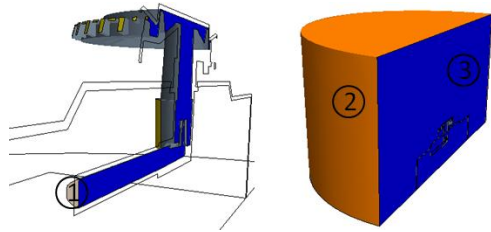
1. Mass Flow Inlet   2. Pressure Outlet
3. Symmetry

Figure 5. Placement of the boundary conditions.

(a) **Nozzle inlet (1):** it was considered the condition of mass flow inlet, the values for this boundary condition was obtained on the experimental tests according to the table 1. The temperature considered was of 300K and the only specie was methane (CH_4).

(b) **Far field surfaces (2):** it was considered the condition of pressure outlet. This condition allowed for the option of backflow in which is allowed for fluid to enter on the domain depending on the pressure gradients. In the case of a back flow it was considered to enter fresh air (M_N=0.79 and M_{O2}=0.21) at 300K.

(c) **Symmetry (3):** for all the surfaces corresponded to the "cut" in the middle of the domain was applied the symmetry boundary condition in which it is considered that all gradients and velocity normal to this plane are zero.

(d) **Other Surfaces:** no slip wall boundary condition was used for momentum equations. Those surfaces are the ones that constitute the walls of the burner and its components responsible to shape the geometry.

Solution Methodology

The numerical study was carried out using the commercial CFD solver, STARCCM+ 10.02 to solve the conservation of mass, momentum and species. This solver uses finite volume method with a polyhedral mesh arrangement to discretize the governing equations.
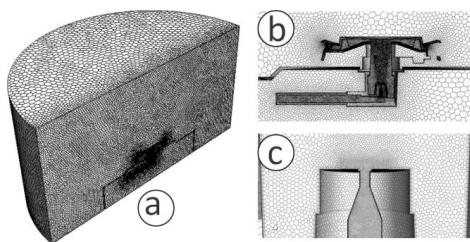

Figure 6. Typical mesh used (a) mesh of the

computational domain (b) mesh on the burner region (c) mesh on the nozzle region.

The velocity and pressure coupling was made using Patankar's (1980) algorithm SIMPLE. The MUSCL scheme (van Leer, 1979) was used for the convective and diffusive terms for both momentum and species equations. The dynamic viscosity was considered to be constant and equal to 1.716e-5 Pa.s, for the molecular diffusivity the Schmidt number used was 1. The thermal conductivity was calculated using the Sutherland's Law (1893), which has a reference value and temperature of 0.02414 W/m-K and 273.15K, respectively with the Sutherland constant of 194K. For both turbulent Prandtl and Schmidt number it was used the software default of 0.9.

RESULTS AND DISCUSSION

In this study, the O_2 concentration values were measured at the ports area, exit, of the burner using a gas analyzer. Also the values of the fuel mass flow was obtained during the tests (table 1). With the two main variables obtained an ANOVA analysis was performed with the software JMP 10, in order to determine the main source of variation as well as an interval of confidence.

Table 1. Values of mass flow (kg/s) used on simulation.

Nozzle diameter (mm)	Mass Flow (kg/s)	Standard deviation
0.64	6.00E-06	2.03E-08
1.10	1.83E-05	2.63E-07
1.60	3.65E-05	4.79E-07
2.00	5.07E-05	8.82E-07

For the mass flow, the analysis showed that the diameter of the nozzle was responsible for 99.9% of the change of this variable, followed by the interation of the burner with the nozzle (0.0427%) then by the burner alone (0.0369%) and finally for the measurement stated as within (0.0009%). The values of the mass flow can be visualized in a chart form on the Fig. 7.
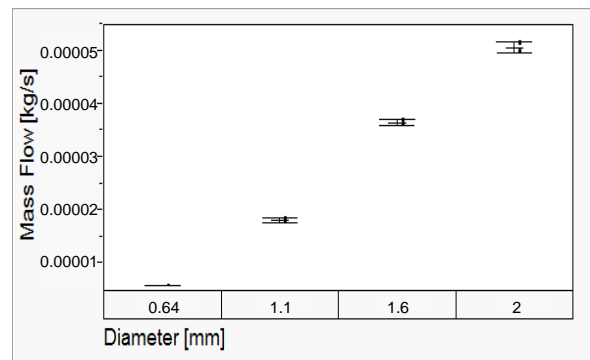

Figure 7. Mass flow value vs nozzle diameter.

The analysis of the O_2 mole fraction was performed in the same fashion. Although the diameter of the nozzle continues to be the main source of variation (77.7%), the contribution of the burner is no more neglected (18.9%), followed by the interaction of the burner with the nozzle (3.2%) and finally for the measurement (0.2313%). The values of the O_2 mole fraction [%] can be visualized in a chart form on the Fig. 8.

The analysis on JMP also allowed for obtain the average standard deviation (σ) considering α=0.05 (software default), that can be observed on the Fig. 9. Considering a normal distribution, for 99.73% of the values to lie within it, the three sigma rule is used (Wheeler & Chambers, 1992), for the interval of confidence is equal the average value of the measurement $\pm 3\sigma$, therefore for this case ± 0.1971.
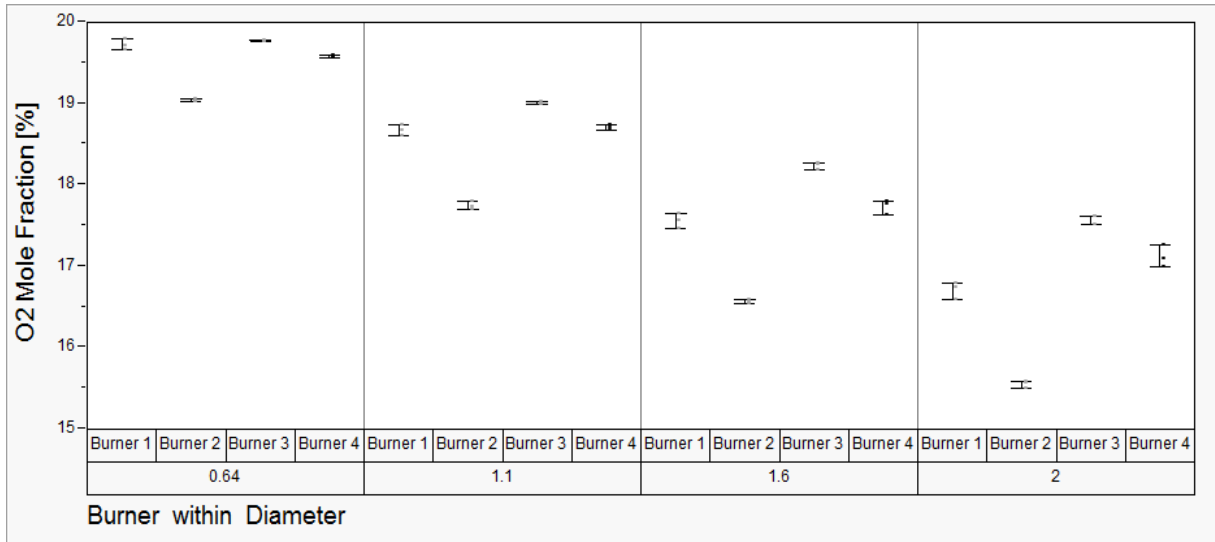

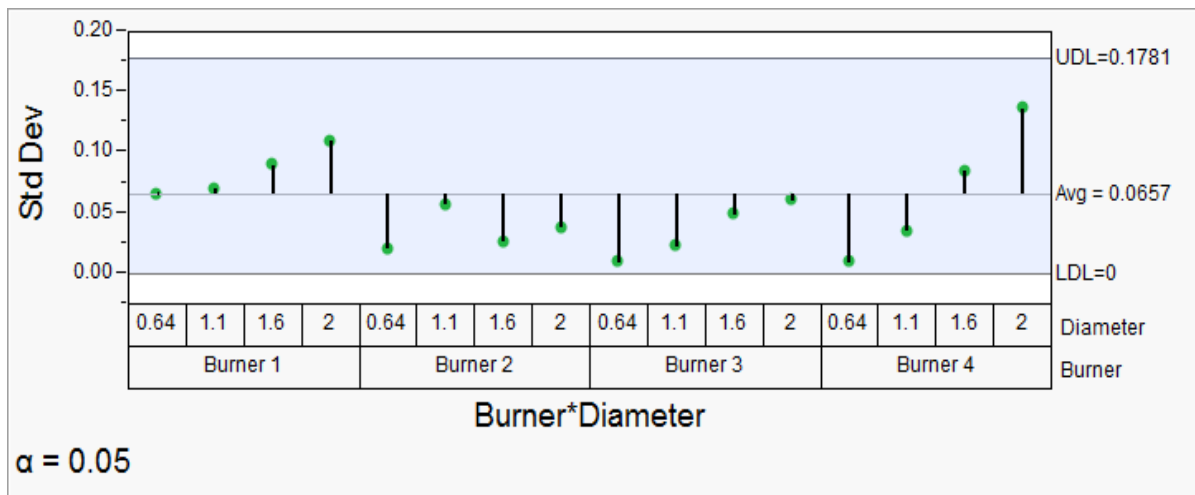Figure 8. O_2 mole fraction [%] per burner and diameter.

Figure 9. Standard deviation for O_2 mole fraction

Knowing that the biggest impact for the O_2 mole fraction is due to the diameter of the nozzle this value was plotted one versus the other, which can be visualized from Figs. 10-14. With those charts one can see that the diameter of the nozzle and the O_2 mole fraction have a linear relation.

The CFD analysis started with the chosen of one burner/nozzle for the mesh refinement test that resulted on the mesh shown in the Fig. 6. For this test the value of O_2 mole fraction was the only data used, once this was the experimental information available. The mesh sizes can be found with the results on Table 2.
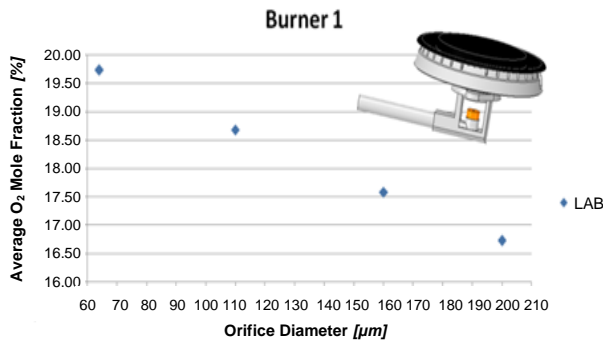
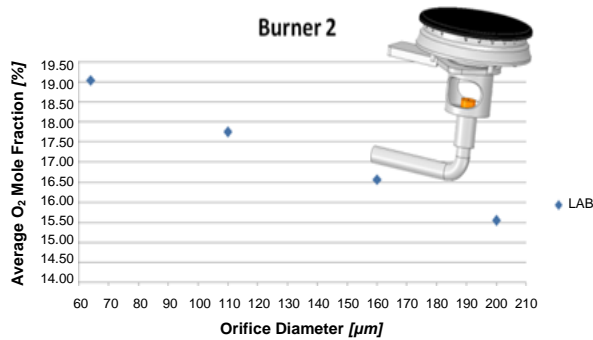Figure 10. Chart O_2 mole fraction vs nozzle diameter for burner 1.

Figure 11. Chart O_2 mole fraction vs nozzle diameter for burner 2.
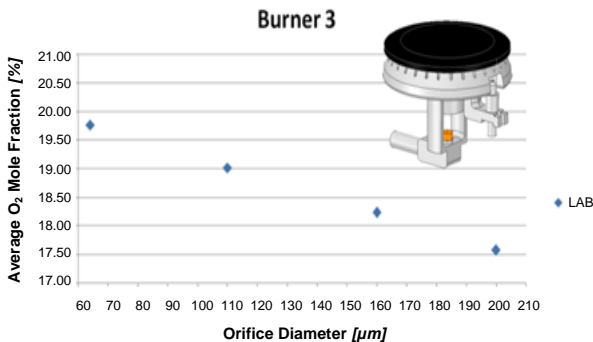

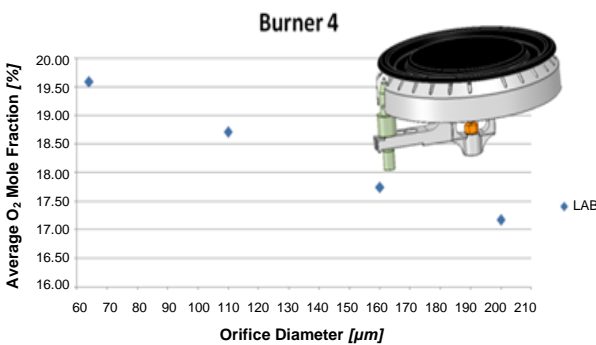Figure 12. Chart O_2 mole fraction vs nozzle diameter for burner 3.

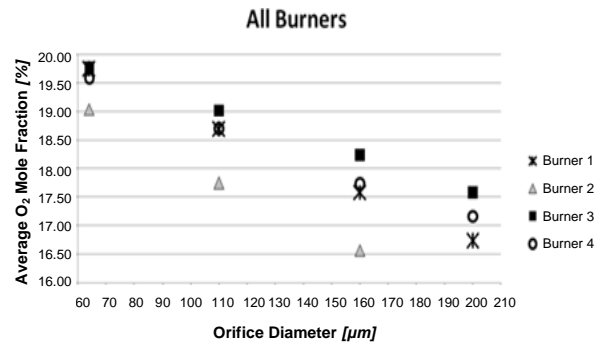Figure 13. Chart O_2 mole fraction vs nozzle diameter for burner 4.

Figure 14. Chart O_2 mole fraction vs nozzle diameter for all burners.

Table 2. Mesh refinement test.

Mesh	Number of Cells	O2 Mole Fraction [%]	Relative Error
Mesh 1	233,999	18.4	0.27
Mesh 2	574,788	18.45	0.03
Mesh 3	2,901,751	18.44	0

Once completed the mesh refinement test all the others geometries were simulated with the corresponded boundary conditions for the mass flow rate. The results can be found on the Tables 3 to 6.

Table 3. CFD results for the burner 1.

d [μm]	LAB	CFD	Abs Diff	% Diff
64	19.73	19.38	0.35	1.79
110	18.68	18.45	0.23	1.24
160	17.58	17.35	0.23	1.31
200	16.73	16.47	0.26	1.54

Table 4. CFD results for the burner 2.

d [μm]	LAB	CFD	Abs Diff	% Diff
64	19.04	18.91	0.13	0.66
110	17.75	17.70	0.05	0.28
160	16.57	16.31	0.26	1.57
200	15.55	15.22	0.34	2.17

Table 5. CFD results for the burner 3.

d [μm]	LAB	CFD	Abs Diff	% Diff
64	19.77	20.03	0.26	1.31
110	19.02	19.01	0.01	0.04
160	18.24	18.26	0.02	0.12
200	17.58	17.60	0.02	0.13

Table 6. CFD results for the burner 4.

d [μm]	LAB	CFD	Abs Diff	% Diff
64	19.58	19.32	0.26	1.32
110	18.70	18.37	0.33	1.79
160	17.74	17.32	0.41	2.32
200	17.17	16.66	0.51	2.95

where:

$$\text{Abs Diff} = \text{abs}(\text{Value}_{LAB} - \text{Value}_{CFD}) \qquad (7)$$

and

$$\% \text{ Diff} = \frac{\text{abs}(\text{Value}_{LAB} - \text{Value}_{CFD})}{\text{Value}_{LAB}} \qquad (8)$$

When compared with the estimated error of 0.1971, only 5 out of the 16 burner configurations have the value from CFD matching the experimental values, being 3 of them for the burner 3. Also one may notice that the biggest deviation occur for the burners 1 and 4. So the deviation may be related to the burner geometry once that for the experimental tests only one burner of each type was tested.

Finally, it is important to emphasize that the maximum error was of 2.95% and considered the complex geometry and all the physical phenomenon that occur inside the burner the turbulence model realizable k-ε presented a good correlation with the experimental data.

CONCLUSIONS

In the present work an experimental and numerical study was conducted to investigate the entrainment in atmospheric burners. The experimental methodology employed was similar to the one presented by A. Namkhat, and S. Jugjai, 2010 and the results compared with the numerical ones. The main conclusions are as follows: (i) the mass flow rate was a function only of the nozzle diameter (ii) the O_2 mole fraction concentration on the ports area presented a linear correlation with the nozzle diameter (iii) most importantly, all the experimental results obtained when compared to the numerical results with the two equation turbulence model realizable k-ε presented a good accuracy (the maximum error was about 2.95%).

ACKNOWLEDGEMENTS

REFERENCES

Carrillo Ibañez, W. A., 2005, Análise e Desenvolvimento de uma Metodologia de Projeto de Queimadores Atmosféricos Tipo Tubo Perfurado, Master Thesis, Universidade Federal de Santa Catarina, Florianópolis, SC. (*in Portuguese*)

CD-Adapco, 2015, *User Guide Star-CCM+*, Version 10.02.

Faveri, R. F., 2013, Avaliação da Transferência de Calor Direta de Chamas Planas Laminares para uma Superfície Isotérmica, Master Thesis, Universidade Federal de Santa Catarina, Florianópolis, SC. (*in Portuguese*)

Field, M. A., Gill, D. W., Morgan, B. B., and Hawksley, P. G. W., 1967, *Combustion of Pulverized Coal Utilization Research Association*, Surrey, England

Glassman, I., and Yetter, R. A., 2008, *Combustion,* 4th Edition, Elsevier Inc., USA.

Kays, W., Crawford, M., and Weigand, B., 2005, *Convective Heat and Mass Transfer*, 4th edition, McGraw-Hill.

Kim, W. H., and Park, T. S., 2013, Effects of Noncircular Inlet on the Flow Structures in Turbulent Jets, Journal of Applied Mathematics and Physics, Vol. 1, No. 6, pp. 37-42.

Namkhat, A., and Jugjai, S., 2010, Primary Air Entrainment Characteristics for a Self-Aspirating Burner: Model and Experiments, Energy, Vol. 35, No. 4, pp.1701-1708.

NBR 13723-1, 2003, *Domestic Cooking Appliance Burning Gas Part 1: Performance and Safety*, Technical Norm, ABNT.

Patankar, S., 1980, *Numerical Heat Transfer and Fluid Flow*, CRC press.

Pritchard, R., Guy, J. J., and Connor, N. E., 1977, *Handbook of Industrial Gas Utilization: Engineering Principles and Practice*.

Shih, T. H., Liou, W. W., Shabbir, A., Yang, Z., and Zhu, J., 1995, A New k-ε Eddy Viscosity Model for High Reynolds Number Turbulent Flows, Computers & Fluids, Vol. 24, No. 3, pp. 227-238.

Singh, G., 1999, Entrainment and Mixing Studies for a Variable Density Confined Jet, Numerical Heat Transfer: Part A, Applications, Vol. 35, No. 2, pp. 205-224.

Singh, G., Sundararajan, T., and Bhaskaran, K. A., 2003, Mixing and Entrainment Characteristics of Circular and Noncircular Confined Jets, Journal of Fluids Engineering, Vol. 125, No. 5, pp. 835-842.

Sutherland, W., 1893, The Viscosity of Gases and Molecular Force, The London, Edinburgh, and Dublin Philosophical Magazine and Journal of Science, Vol. 36, No. 223, pp. 507-531.

Van Leer, B., 1979, Towards the Ultimate Conservative Difference Scheme. V. A Second-Order Sequel to Godunov's Method, Journal of Computational Physics, Vol. 32, No. 1, pp. 101-136.

Wheeler, D. J., and Chambers, D. S., 1992, *Understanding Statistical Process Control,* SPC Press.

Wilcox, D. C., 1998, Turbulence Modeling for CFD, La Canada CA: DCW Industries, Vol. 2, pp. 103-217.